VORTEX STRUCTURE OF A WAKE BEHIND A SPHERE IN A STRATIFIED FLUID

E. Ya. Sysoeva and Yu. D. Chashechkin

UDC 532.527

The dynamics of the formation of vortices in the flow of a uniform fluid about a two-dimensional body has been studied in fairly great detail both theoretically (by analytical and numerical methods) and experimentally [1-3]. Less attention has been given to the vortex structure of flow behind a three-dimensional body. According to asymptotic solutions, a stationary vortex is created in the aft region of a sphere at Reynolds numbers Re > 20 [1]. The structure of this vortex in a uniform fluid was studied experimentally in [4]. At 130 < Re < 300, the vortex pulsates, and it begins to separate from the body at Re > 400. The separation of isolated vortices from a sphere was visualized in [5]. Vortex flow behind a sphere in a nonuniform fluid was studied by the tinting method in [6] (three tests were conducted altogether). A series of vortices similar to a Karman street behind a cylinder was observed in the horizontal plane. The dye was distributed in two separate layers in the vertical plane, which is indicative of splitting of the flow behind the body. With the assumption that the stratification had little effect, a model of vortex flow was constructed which consisted of two intersecting spiral vortex tubes. Isolated vortices with a vertical symmetry axis are formed at the points of contact of the tubes. The value of the Strouhal number Sh increases from 0.14 (Re = 4300) to 0.22 (Re = 17,400), with $Sh = nd/U_0$, where d and U_0 are the diameter and velocity of the sphere and n is the frequency of vortex shedding. It has been established by numerical methods that stratification has a significant effect on the character of flow about a body and the structure of the boundary layer [7]. It has been shown experimentally that the thicknesses of the viscous and dense boundary layers in a fluid with salt stratification do not coincide [8]. Vorticity can be transferred in a nonuniform fluid not only by individual vortices, but also by internal waves. More types of wake structures can exist in a stratified medium than in a uniform medium due to the development of Taylor instability (when a heavier fluid turns out to be above a lighter fluid) and Kelvin–Helmholtz instability (when the velocity shift is greater than the buoyancy frequency). The degree to which these structures are manifest depends on the relationship of the acting forces. In particular, the formation of discrete vortices may be connected with the generation of vorticity both in the vicinity of the body and on the boundary of the wake, in the zone of maximum gradients of density and velocity shift. No systematic study has been made of a vortex flow structure behind a three-dimensional body in a stratified medium. The goal of the present study is to experimentally investigate the vortex structure of a wake behind a sphere moving horizontally with a constant velocity in a fluid with a linear density distribution. The method of shadow visualization is used to determine the types of vortex structures that might develop and the conditions of their formation.

Experiments were conducted in a basin 1.5 m long, 0.4 m wide, and 0.46 m high. The basin was filled layer by layer with an aqueous solution of common salt with a variable concentration. The buoyancy period was measured by the method of density marking [9]. The flow pattern was recorded with an IAB-451 shadowgraph. In most of the tests, the body being towed was secured to a Nichrome wire 0.15 mm in diameter. We studied flows behind spheres of the diameter d = 0.5, 1.0, and 2.0 cm in a fluid with a buoyancy period T_k = 4.1 sec. Here, Λ = 420 cm. The velocity of the body was no greater than 7 cm/sec. All of the measurements were made in the middle part of the basin, where the velocity of the model was kept constant. The experimental method is explained in more detail in [8]. The geometric characteristics of the flows were measured from shadowgrams with the aid of a Stecometer comparator (German Democratic Republic). The coordinates of the boundaries of the flows were recorded in digital form with an instrument error of 0.002 mm. The error was 0.03 mm with allowance for the scale of the measurements.

The characteristic dimensional parameters of the problem were as follows: body diameter d, body velocity U_0, kinematic viscosity ν, acceleration due to gravity g, buoyancy scale

Moscow. Translated from Zhurnal Prikladnoi Mekhaniki i Tekhnicheskoi Fiziki, No. 2, pp. 40-46, March-April, 1986. Original article submitted February 15, 1985.

0021-8944/86/2702-0190$12.50

$\Lambda = [\partial \ln \rho / \partial z]^{-1}$. The natural time scale was the buoyancy period T_k (frequency N). Here, $T_k = 2\pi/N = 2\pi\sqrt{\Lambda/g}$. The dimensionless characteristics were as follows: Reynolds number $Re = U_0 d/\nu$, scale ratio $C = \Lambda/d$, internal Froude number $Fr = U_0^2/N^2d^2$ [10].

Seven characteristic types of wakes can be distinguished from the results of tests conducted behind a sphere moving horizontally in a stratified fluid: a laminar wake with rectilinear boundaries; a laminar wake with a conical internal structure; a pulsating wake (laminar with wavy boundaries); a wave-vortex wake (with small vortices on the periphery of the wake); a nonsteady-vortex wake (a vortex commensurate with the size of the body is periodically formed behind the body); a vortex wake (the wake is a vortex street); a turbulent wake.

We will examine each of these regimes in more detail. As in a uniform fluid, flow in the wake is laminar in character at low velocities of the sphere. A layer of fluid with a density gradient greater than the initial value is formed in the stratified fluid at the periphery of the wake. This is the density boundary of the wake, and the degree to which it is manifest (the maximum value of gradρ) and its extent (the distance from the sphere over $|\text{grad}\,\rho| > |\text{grad}\,\rho_0|$ within the sensitive range of the shadowgraph) increases with an increase in the diameter of the sphere and stratification. The density boundary appears on the shadowgrams in the form of thin dark bands which approach the points of flow separation from the sphere (Fig. 1a, $T_k = 4.2$ sec, d = 2 cm, $U_0 = 0.68$ cm/sec). Its length is 0.66d for spheres of the diameter d = 0.5 and 1 cm and 1.2d for spheres with d = 2.0 cm, $T_k = 4.2$ sec. The density boundary is located at the center of the region of maximum shift of the velocity of the wake ($\partial u_x/\partial z$) at the wake's periphery, which is visualized in Fig. 1a with the aid of a density marking. It follows from analysis of shadowgrams with density markings that the thickness of the layer in which there is an abrupt change in density $\delta = 36$ mm (the relative error of the measurements is ±20%). This value is 17 times smaller than the width of the velocity-shift layer. The velocity profile of the wake is smooth, in this regime, and the maximum lies on the wake axis. Laminar flow about the sphere was seen at velocities below $U_0 = 1.7$ cm/sec for the sphere with d = 0.5 cm ($Re \leq 85$, $Fr \leq 4.9$), at $U_0 \leq 0.95$ cm/sec when d = 1 cm ($Re \leq 95$, $Fr \leq 0.39$), and at $U_0 \leq 0.68$ cm/sec when d = 2 cm ($Re \leq 136$, $Fr \leq 0.048$).

All of the photographs in Fig. 1 show a visualization of the flow pattern near the vertical plane passing through the line of motion of the body. The photographs were obtained by the method of a vertical slit — a Foucault knife-edge. The changes in density of the darkening are proportional to variations in the horizontal component of the gradient of the refractive index in the direction of motion of the body. The diffuse dark and light bands (semicircles behind the body outside the wake and inclined diffuse bands inside the wake) are the attached and captured internal waves described in [8].

With an increase in velocity, the external boundary of the laminar wake ceases to be rectilinear and splits into filaments which diverge in the form of individual cones enclosed in each other. Such flow is seen behind the sphere with d = 0.5 cm in the velocity range $1.7 < U_0 \leq 3.4$ cm/sec ($85 < Re \leq 170$, $0.048 \leq Fr \leq 20.1$) (no tests were conducted at high velocities) and behind the sphere with d = 1.0 cm at $0.95 < U_0 < 1.74$ cm/sec ($95 < Re < 174$, $0.39 < Fr < 1.29$). The wake contracts to 0.15d immediately behind the sphere and then expands to the diameter of the sphere at the distance 5-6d.

With an increase in velocity, the wake behind the large-diameter sphere is transformed from a laminar to a pulsating wake, with wavelike gradients. This regime is seen behind the sphere with d = 2 cm in the velocity range $0.68 < U_0 < 1.62$ cm/sec ($136 < Re < 324$, $0.048 < Fr < 0.28$ (Fig. 1b, d = 2 cm, $U_0 = 1.08$ cm/sec). The wake expands to 0.75d at a distance 0.8-0.9d from the sphere. Meanwhile, the distance of the region of maximum expansion of the wake increases with an increase in velocity. The wake then contracts to 0.4d at the distance 2d. A small vortex with a horizontal rotation axis can be seen in the region of maximum wake expansion, the formation of this vortex being connected with the development of Kelvin–Helmholtz instability on the wake boundary in the zone of the maximum velocity shift and density gradient.

A stagnation zone bounded by layers with steep velocity gradients is seen in the velocity range $1.74 \leq U_0 \leq 4.5$ cm/sec ($174 \leq Re \leq 450$, $1.29 \leq Fr \leq 8.65$) after the sphere with d = 1.0 cm and in the range $1.62 < U_0 < 2.36$ cm/sec ($324 < Re < 472$, $0.28 < Fr < 0.59$) after the sphere with d = 2.0 cm. The boundary of the zone is not smooth, and small-scale vortical disturbances with dimensions on the order of the thickness of the density boundary layer are formed on it. These vortices periodically separate and form a typical stepped wake structure (Fig. 1c — d = 1.0 cm, $U_0 = 3.13$ cm/sec; Fig. 1d — d = 2.0 cm, $U_0 = 2.36$ cm/sec). The vorti-

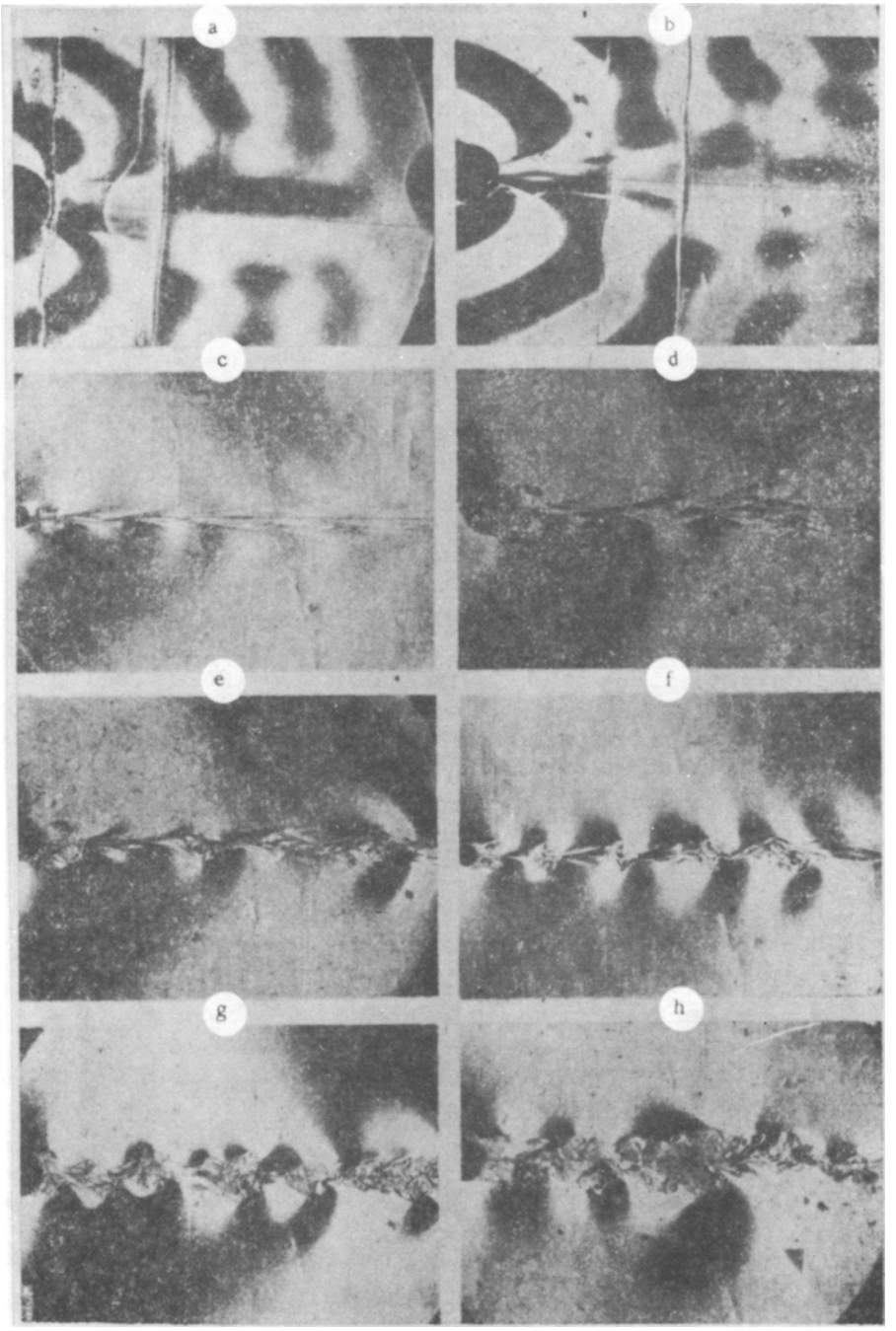

Fig. 1

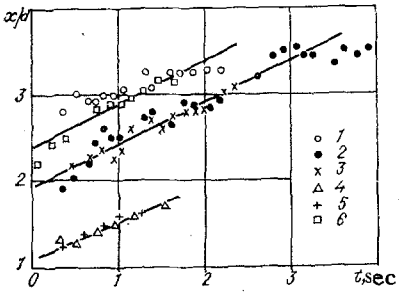

Fig. 2

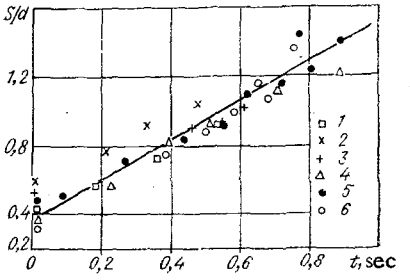

Fig. 3

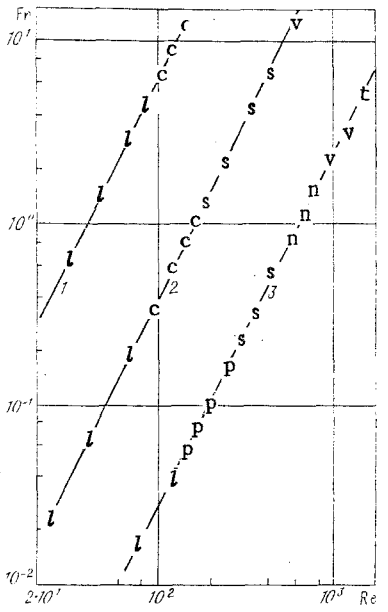

Fig. 4

cal motion produces abrupt variations in the refractive index, and these small vortices are quite visible on the shadowgraphs. The development of instability is actually observed in the density wake, which is much thinner than the velocity-shift layer and the width of the wake as a whole. After separation, the vortices rapidly flatten out in the vertical direction under the action of buoyancy, spread out in the horizontal direction and, disintegrating, stretch out into thin streaks which gradually smooth the external boundary of the wake. The horizontal dimension of such vortices increases linearly with time at the rate 5-7 mm/sec, depending on the velocity of the sphere. The vertical dimension of the vortices ℓ_z decreases with time at the rate 0.9 mm/sec at $t > 0.4$ sec when the velocity of the body $U_0 = 1.78$ cm/sec. For $U_0 = 2.36$ cm/sec, the vertical dimension increases somewhat with time at $t < 0.8$ sec and then decreases at a rate of 1.1 mm/sec in the range $0.8 \leq t \leq 1.6$ sec and at the rate 3.5 mm/sec at $t > 1.6$ sec. The lifetime of the vortices is short and amounts to 2-2.5 sec according to the shadow observations. The lifetime of the layered structure after disintegration of the individual vortices at the periphery of the wake is 4-5 sec.

Using the laboratory coordinate system, we determined the dependence on time t of the horizontal distances between vortices normalized on the diameter of the sphere x/d. These results are shown in Fig. 2, where 1 is the distance between the first and second vortices with the motion of the sphere with d = 1.0 cm at the velocity $U_0 = 2.23$ cm/sec. The numbers 2 and 3 denote the distances between the second and third and third and fourth vortices, respectively, for the same sphere. The numbers 4 and 5 denote the distances between the third and fourth vortices and the fourth and fifth vortices, respectively, for the sphere with d = 2.0 cm, $U_0 = 2.36$ cm/sec. The number 6 is for d = 1.0 cm, $U_0 = 4.5$ cm/sec. It is evident that these distances increase on the average in proportion to the time. Meanwhile, the rate of increase v = 0.48 mm/sec is independent of the diameter and velocity of the sphere. The nonmonotonic nature of the change in distances is connected with the internal dynamics of the vortices, leading to a change in their dimensions and form.

Subsequent increase in velocity leads to an increase in the intensity of vortical motion in the bottom part of the sphere. Meanwhile, the thickness of the vortex shell (the boundaries of the vortex with a high density gradient) is determined by the thickness of the relatively thin density boundary layer (the layer of fluid near the surface of the body in which the density gradient is greater than the initial gradient) at the point of its separation from the body. At the stage of vorticity accumulation, the density irregularities (curves) in the wake directly behind the sphere form the characteristic spiral structure, similar to the internal structure of the streamlines of a free laminar toroidal vortex ring. When the size of the vortical stagnation zone approaches its greatest value, the flow inside it becomes unstable and small-scale mixing occurs — possibly as a result of Taylor instability. The vortexlike structure ("cloud," "puff") periodically separates from the body and rapidly disintegrates into a system of curves stretched out in the direction of mean velocity. The lifetime of these structures is no greater than 1 sec. This regime is seen in the wake behind the 2-cm-

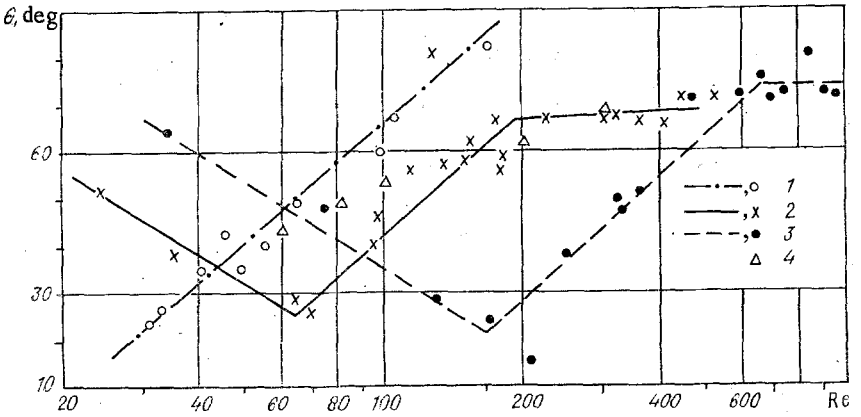

Fig. 5

diameter sphere at the velocities $2.87 \leq U_0 \leq 3.43$ cm/sec, $574 \leq Re \leq 686$, $0.88 \leq Fr \leq 1.26$, and is shown in Fig. 1e.

Figure 3 shows the horizontal dimension of a transient stagnation zone normalized on the diameter of the sphere s/d from the moment of its formation to separation; here, points 1 correspond to the velocity of the sphere $U_0 = 3.34$ cm/sec; 2 and 3 correspond to $U_0 = 3.43$ cm/sec (we followed the behavior of two successive zones); 4 to $U_0 = 3.68$ cm/sec, 5 to $U_0 = 4.2$ cm/sec, and 6 to $U_0 = 4.6$ cm/sec; this dimension increases in proportion to the time $s/d = \alpha t + 0.4$, $\alpha = 1.1$ sec^{-1} and is independent of the velocity of the body. In the coordinate system connected with the fluid, the outermost point of the stagnation zone during its formation moves at a constant velocity of 2.1 cm/sec in the direction of motion of the body.

Vortical motion in the bottom part becomes more stable when the sphere is moving at high velocities. The vortical stagnation zone behind the sphere periodically separates and exists in the wake in the form of circular vortices connected with each other by thin layered loops. The vortex ring envelops the line of motion, and its bottom edge is inclined somewhat toward the motion. The vortex loops connecting the circular vortices are inclined at one angle $\alpha = 20°$ to the line of motion. This regime is seen with motion of the sphere d = 1 cm, $U_0 = 5.4$ cm/sec (Fig. 1f) (no tests were conducted at high velocities) and d = 2 cm, $3.68 < U_0 < 5.8$ cm/sec (Fig. 1g, $U_0 = 5.2$ cm/sec). The lifetime of the individual vortices is 5-6 sec. They flatten under the action of buoyancy, stretch out in the direction of mean velocity, and merge into a single wake consisting of discrete high-gradient layers. During its motion, each circular vortex emits its own system of attached internal waves. The vertical dimension of the vortices is unstable over time. The period of oscillation of this dimension is about 4 sec and is comparable to the buoyancy frequency $T_k = 4.1$ sec. The horizontal distance between vortices increases somewhat during the first second and thereafter remains nearly constant, depending slightly on the velocity of the sphere. The velocity of the vortices is about 4.5 mm/sec and changes little over time. It should be noted that the error of measurement of the parameters of the vortex structures in this regime is fairly large (20-25%). This is connected on the one hand with the development of small-scale instability in the internal flow, leading to blurring of the boundaries of the vortices. It is due on the other hand to the internal dynamics of the flow (flattening and spreading).

A further increase in velocity ($U_0 \geq 7$ cm/sec, d = 2 cm) produces a turbulent wake (see Fig. 1h). Turbulence may occur in the wake as a result of the agitation and coalescence of individual vortices, intensive development of Kelvin–Helmholtz instability in the region of abrupt expansion of the wake, and agitation of the boundary layer on the body. One or several of these factors, acting simultaneously, may be decisive, depending on the amount of stratification and the dimensions of the body. In the present case, discrete vortex structures undergo agitation and disintegration.

The set of flow regimes investigated is shown in an Fr–Re diagram (Fig. 4) constructed in double-log coordinates. In these variables the data corresponding to spheres of different diameter lies on straight lines with the slope k = 0.5; 1-3 correspond to d = 0.5, 1, and 2 cm; the letter ℓ denotes conditions under which a laminar wake is seen, c denotes a laminar wake with a conical internal structure, p denotes a pulsating wake, s denotes the regime of small vortices at the periphery of the wake, n denotes a nonsteady-vortex wake, v denotes a vortex wake, and t denotes a turbulent wake. Stratification stabilizes the flow considerably, and a laminar wake is present at $Re < 90$, d = 0.5 and 1.0 cm and $Re < 240$, d = 2.0 cm

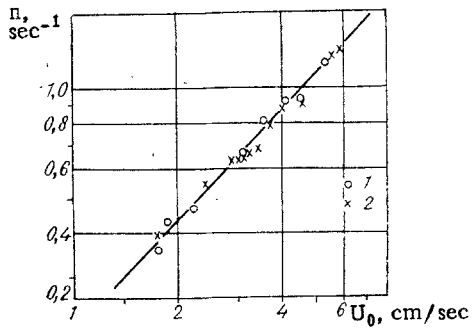

Fig. 6

compared to Re < 24 for a uniform fluid. It follows from the data shown that the boundary of instability of laminar flow is shifted slightly toward large Re with an increase in diameter. This tendency remains with a further increase in the diameter of the sphere. The flow conditions are appreciably more dependent on the internal Froude number. The ratio of values of the critical Fr at the end of the laminar regime is 115:7:1 for spheres with d = 0.5, 1.0, and 2.0 cm, respectively. This is greater than the value of the ratios resulting from an increase in diameter (16:4:1). The boundaries between all of the flow regimes are shifted toward larger Re with an increase in sphere diameter.

The stabilizing effect of stratification is also manifest in the dependence of the angle θ (the angle of flow separation on the sphere) on Re, shown in Fig. 5. The angle is reckoned from the line of motion ($\theta = 90°$ when the flow separates on a principal transverse diameter); 1-3 correspond to d = 0.5, 1.0, and 2.0 cm, while 4 corresponds to tests in a uniform fluid [4]. In a uniform fluid behind spheres with d = 1.5 and 1.9 cm, the value of the angle monotonically increases from 45 to 70° with an increase in Re from 60 to 300, regardless of the sphere diameter. In a stratified fluid, the behavior of the separation angle for spheres of different diameter is qualitatively similar. Separation of laminar flow from the surface of the sphere occurs with $\theta = 50°$ when d = 1.0 cm and with $\theta = 65°$ when d = 2.0 cm. The point of separation is shifted toward the line of motion with an increase in velocity in the conical-wake regime. The minimum angle of separation $\theta = 24°$ for d = 0.5 cm, $\theta = 25°$ for d = 1.0 cm, and $\theta = 15°$ for d = 2.0 cm. With a further increase in velocity, vorticity accumulates in the bottom part of the sphere and the separation point begins to shift toward the external diameter. The maximum value of the separation angle $\theta = 80°$ when d = 2 cm. The dependence of the angle of separation on the Reynolds number can be approximated as $\theta \cong b \log \mathrm{Re}$, where b = −0.9 at d = 1 cm (25 < Re < 65) and d = 2.0 cm (35 < Re < 180); b = 0.9 at d = 1.0 cm (65 < Re < 200) and d = 2.0 cm (180 < Re < 800). When Re > 200 with d = 1 cm and Re > 600 with d = 2.0 cm, the separation angle slowly changes with an increase in velocity and Re. The dependence of the separation angle on the Froude number is similar in character. The minimum separation angle is achieved at Fr = 0.19 and 0.11 for d = 1.0 and 2.0 cm, respectively.

Figure 6 shows the dependence of the frequency of shedding n of all types of vortices investigated on the velocity of the sphere U_0. Here, the numbers 1 and 2 correspond to d = 1 and 2 cm, respectively. All of the points lie on one straight line in double-log coordinates. The shedding frequency is proportional to the velocity of the body. Accordingly, the Strouhal number Sh in the range $10^2 < \mathrm{Re} < 10^3$ takes a value of 0.2 for the sphere with d = 1.0 cm and 0.4 for d = 2.0 cm. In a uniform fluid, according to the measurements in [5], Sh is independent of the sphere diameter and increases from 0.15 to 0.5 with a change in Re from 400 to 1000.

LITERATURE CITED

1. M. Van Dyke, Perturbation Methods in Fluid Mechanics, Parabolic Press (1975).
2. L. D. Landau and E. M. Lifshitz, Fluid Mechanics, Pergamon (1959).
3. U. R. Prupapacher, B. P. LeClair, and A. E. Hamielec, "Some relations between drag and flow pattern in viscous flow past a sphere and a cylinder at low and intermediate Reynolds numbers," J. Fluid Mech., 44, Pt. 4 (1970).
4. S. Taneda, "Experimental investigation of the wake behind a sphere at low Reynolds numbers," Rep. Res. Inst. Appl. Mech. Jpn., 4, No. 16 (1956).
5. E. Achenback, "Vortex shedding from spheres," J. Fluid Mech., 62, Pt. 2 (1974).
6. H.-P. Pao and T. W. Kao, "Vortex structure in the wake of a sphere," Phys. Fluids, 20, No. 2 (1977).

7. L. I. Turchak and V. P. Shidlovskii, "Equations of motion of a stratified fluid," Dokl. Akad. Nauk SSSR, 254, No. 2 (1980).
8. Yu. D. Chashechkin, A. A. Makarov, and V. S. Belyaev, "Attached internal waves," Preprint IPM Akad. Nauk SSSR, No. 214 (1983).
9. V. I. Nekrasov and Yu. D. Chashechkin, "Measurement of the velocity and period of free internal oscillations of a fluid by the method of density markings," Metrologiya, No. 11 (1974).
10. Yu. D. Chashechkin, "Characteristics of submerged turbulent jets in nonuniform fluids," FAO, 10, No. 12 (1974).

MODEL OF THE PENETRATION OF AN UPPER UNIFORM LAYER INTO A STRATIFIED FLUID

V. Yu. Lyapidevskii

UDC 532.526;551.465

We study an integral model of the penetration of a uniform layer of fluid under the action of a tangential stress applied to the surface. The conservation equations for mass, momentum, and energy are closed by the penetration law of the nonmoving fluid into the upper uniform layer. An important feature of our model is that the nonuniformity of the velocity field due to the presence of "free" vortices in the flow is taken into account.

Two penetration regimes are identified: a subcritical regime, where the penetration of the fluid into the layer occurs because of externally induced turbulence of the uniform layer, and a supercritical regime in which turbulence at the surface is transported by large-scale vortices generated by a flow instability with a velocity shear. It is shown that for an initial bilayered density distribution, and also in the case of a continuous density distribution following a power law, there exist singular solutions of the system of equations corresponding to the supercritical penetration regime, and these solutions determine the asymptotic behavior at large times. These solutions are characterized by the constancy of the global Richardson number Ri_u, calculated with respect to the mean values of the buoyancy and velocity of the upper layer. Hence the hypothesis Ri_u = const used in several models [1] to close the momentum equation is correct asymptotically in the framework of our model. Inclusion of the lateral friction for flow in a channel of finite width destroys the asymptotic form of the penetration and the solution is transformed into the subcritical regime. Comparison with experimental results in circular troughs shows that our model gives a satisfactory description of the supercritical penetration for a bilayer [2] and for a continuous initial density distribution [3].

The process of mixing in the flow of a stably stratified fluid is a complex and important problem. Transport of momentum and heat from the surface into the bulk of the ocean determines the formation and time behavior of the upper thermocline. The transport mechanism is related to the development of instabilities in the shear flow and to turbulent exchange between layers of different densities. An adequate mathematical description of the formation and structure of the upper layer of the ocean is possible only with the use of turbulent models [4]. However, for a certain class of flows a simple integral model can be used which gives the time behavior of the average quantities, which completely characterize this class of flow.

In experiments and in observations it is noted that a stress applied to the surface of a stratified fluid at rest leads to a well-mixed layer with a nearly constant velocity and density and the layer is separated from the unperturbed nonmoving fluid by a thin transition layer where there are large gradients. In an idealized formulation of the problem, one assumes that the layer is uniform and has density $\rho(t)$, and a horizontal component of the velocity $u(t)$ (the only component which is nonzero), and the small-scale motion extends to a depth $h(t)$ with intensity $q(t)$ (Fig. 1, region I). Below the line $y = -h(t)$ there is the nonmoving

Novosibirsk. Translated from Zhurnal Prikladnoi Mekhaniki i Tekhnicheskoi Fiziki, No. 2, pp. 47-52, March-April, 1986. Original article submitted December 28, 1984.

0021-8944/86/2702-0196$12.50